ChemComm

Accepted Manuscript

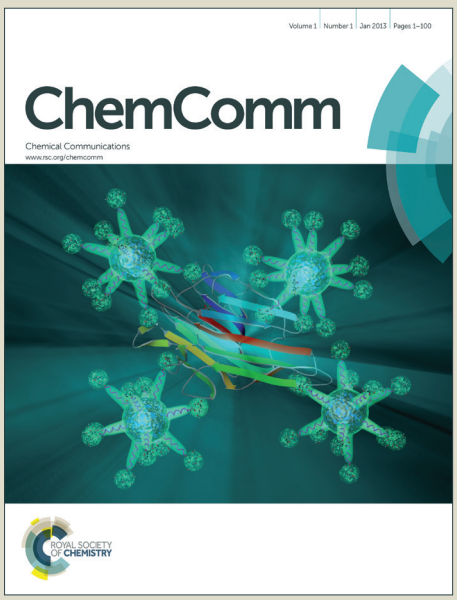

ROYAL SOCIETY OF CHEMISTRY

www.rsc.org/chemcomm

Journal Name

RSCPublishing

COMMUNICATION

A sputtered CdS buffer layer for co-electrodeposited Cu_2ZnSnS_4 solar cell with 6.6% efficiency

Cite this: DOI: 10.1039/x0xx00000x

Jiahua Tao,[a] Kezhi Zhang,[a] Chuanjun Zhang,[b] Leilei Chen,[a] Huiyi Cao,[a] Junfeng Liu,[a] Jinchun Jiang,[b] Lin Sun,[a]* Pingxiong Yang[a] and Junhao Chu[ab]

Received 00th January 2012,
Accepted 00th January 2012

DOI: 10.1039/x0xx00000x

www.rsc.org/

Cu_2ZnSnS_4 thin films with thicknesses ranging from 0.35 to 1.85 µm and micron-sized grains (0.5-1.5 µm) were synthesized using co-electrodeposited Cu-Zn-Sn-S precursors with different deposition times. Here we have firstly introduced a sputtered CdS buffer layer for the development of CZTS solar cells, which enables breakthrough efficiencies up to 6.6%.

Chalcogenide-based thin film photovoltaic material Cu_2ZnSnS_4 (CZTS) has recently attracted significant interest as a potential candidate for the massive production of solar cells at large scale, because CZTS is composed of the earth-abundance and non-toxicity of the constituent elements. It has a near-optimum direct band gap of approximately 1.5 eV, a large absorption coefficient over 10^4 cm^{-1}, and the rapid improvement in power conversion efficiency (PCE).[1-3] The theoretical PCE of single junction CZTS device is 32.4% with J_{sc}=29.6 mA cm^{-2}, V_{oc}=1.21 V and FF=89.9%, according to the Shockley-Queisser efficiency limit.[4] However, even the $Cu_2ZnSnS_xSe_{4-x}$ (CZTSSe) world record efficiency of up to 12.6% is still far below the theoretical limit.[5] Thus, obviously there is still plenty of room to make substantial progress towards developing low-cost and high-efficiency photovoltaic devices.

CZTS solar cells have been prepared by vacuum-based-deposition, such as co-evaporation and sputtering processes, and have achieved PCEs of 8.4%[6] and 6.77%,[7] respectively. Several non-vacuum-based-deposition techniques, such as a hydrazine-based precursor solution approach,[3,5] sol-gel method,[8,9] spray pyrolysis[10] and electrodeposition[2,11-14] are also being developed for preparing high efficiency CZTS devices. Among them, electrodeposition is an attractive non-vacuum growth process due to its technical advantages for the fabrication of low-cost solar cells. For instance, its inexpensive equipment has been commercially used in the fabrication of semiconductor chips on printed circuit boards, it is easily exploited in industry on large-area substrates and electrolytes are prepared from environmentally friendly and low-cost solutions. Moreover, there is no need to use toxic solvents or ligands like hydrazine.[3,5] In the pioneering work reported by Ennaoui et al, a CZTS solar cell prepared by co-electrodeposited Cu-Zn-Sn precursor followed by sulfurization in H_2S atmosphere at 550 °C for 2 h achieved a PCE of 3.4%.[12] However, the major drawback of this method reported in the literature is the use of highly toxic H_2S instead of sulfur powder, which is unsuitable for an industrial process in terms of both environment and security. Ahmed et al. reported a PCE of 7.3% using a CZTS based solar cell prepared by preheating of an electrodeposited Cu/Zn/Sn metallic stack followed by sulfurization at 585 °C for 12 min.[2] Thus far, the champion record based on stacked electrodeposition has reached a PCE of 8% for CZTS solar cells, which were fabricated by sulfurization of preheated Cu/Zn/Sn metallic stack precursors at 590 °C for 10 min.[11] Previously, we have reported that CZTS solar cells can be co-electrodeposited using different deposition potentials, yielding a PCE of 3.68%.[13] Compared to the stacked electrodeposition, co-electrodeposition process greatly simplifies the fabrication process of the CZTS precursor. In this report, a champion co-electrodeposited CZTS solar cell with a PCE of 6.6% is fabricated.

Generally, the cadmium sulfide (CdS) with a large bandgap of 2.4 eV is the most promising buffer layer for the CZTS/CdS heterojunctions in devices, and the highest conversion efficiencies have been achieved using the chemical bath deposition of CdS thin films (CBD-CdS thicknesses in the range of 25-120 nm[2-9,11-15]). However, the n-type CdS layer deposited by CBD causes some serious environmental problems due to the large amount of cadmium-containing waste during the CBD process. In this regard, we present radio-frequency (RF) sputtering to process CdS layer, which is suitable to reduce the environmental impact and can enhance the continuity of the deposition processes so that thin film solar cells can be manufactured by an in-line process for massive production. So far, the sputtered CdS buffer layer for a CZTS solar cell in device performance has not been demonstrated. In this work, we have systematically studied the influence of deposition time on the properties of CZTS thin films, and have demonstrated the successful use of a sputtered CdS buffer layer for CZTS based solar cells with efficiencies as high as those fabricated using CBD-CdS.[2,4,8] The results offer new research directions for solving persistent challenges of CBD-CdS in CZTS photovoltaics.

Fig. 1a shows XRD patterns of all films derived from sulfurization of precursors co-electrodeposited for various durations. Besides the diffraction peak from Mo substrates, the main peaks of the sulfurized CZTS films at approximately 2θ=18.20, 28.53, 32.98, 47.33 and 56.17° match very well with the diffraction of the (101), (112), (200), (220) and (312) crystal planes of the kesterite structure

CZTS (JCPDS 26-0575) with a preferred grain orientation along (112) direction.[4] The intensity of all diffraction peaks becomes relatively more intense and sharper with increasing the deposition time, indicating the expected increases in crystalline with larger grains (Fig. 2). However, it should be noted that XRD diffraction peaks cannot unambiguously distinguish other common secondary phases such as ZnS and Cu_2SnS_3.

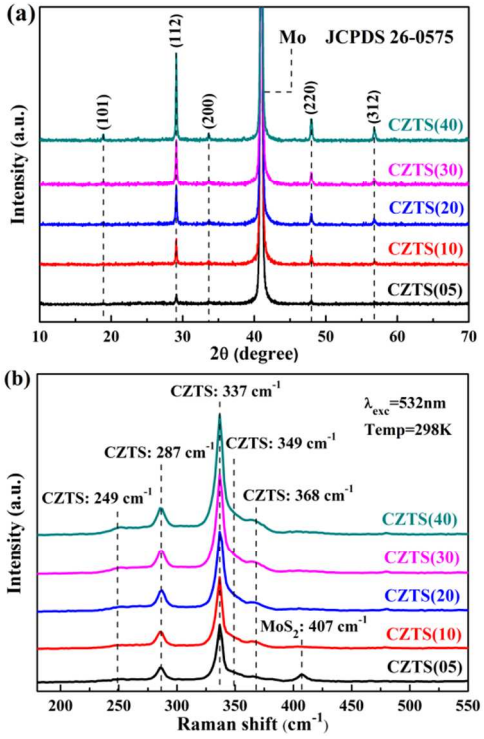

Fig. 1(a) XRD patterns and (b) Raman spectra of the sulfurized CZTS films deposited for different durations.

Therefore, Raman spectroscopy was utilized to obtain further the phase identification, and the results of the CZTS films are compared in Fig. 1b. All CZTS films exhibit the main peaks at 249, 287, 337, 349 and 368 cm^{-1}, which can be assigned to kesterite CZTS structure.[9] Raman spectra also reveal the presence of MoS_2 with an extremely weak peak at around 407 cm^{-1} in the CZTS(05) film from the relatively short deposition time,[13] but no layer could be resolved by SEM. Besides, the MoS_2 Raman signal for the CZTS(10, 20, 30 and 40) films from the relatively long deposition times is not observed, this can be explained by the fact that the effective penetration depth of the Raman scattering technique with the excitation wavelength 532 nm is limited and a MoS_2 layer at bottom layer near thicker CZTS films possibly may not be detected by 532 nm laser. No unidentified secondary phases are observed by either XRD or Raman measurements, demonstrating well-crystallized and single phase CZTS films.

Fig. 2 shows surface and cross-sectional SEM images of the sulfurized CZTS films. It is clear that there are notable differences in grain sizes ranging from 0.5 μm for CZTS(05), 0.8 μm for CZTS(10), 1.1 μm for CZTS(20), 1.2 μm for CZTS(30) to 1.5 μm for CZTS(40). The longer the deposition time, the larger the grain size. It implies the significant improvement of the grain size of CZTS thin films, which is consistent with XRD and Raman spectrum analyses. Large grains generally benefit device performance due to less opportunity for recombination of photogenerated carriers at the grain boundaries.[2] Moreover, the surface roughness of the films seem to show the same trend: the longer the deposition time, the rougher the film surface. This result is expected as larger grain size normally results in rougher surface. The relatively flat surface films may be beneficial to the formation of CZTS/CdS heterojunction and thus reduce the interface combination of charge carriers.[13]

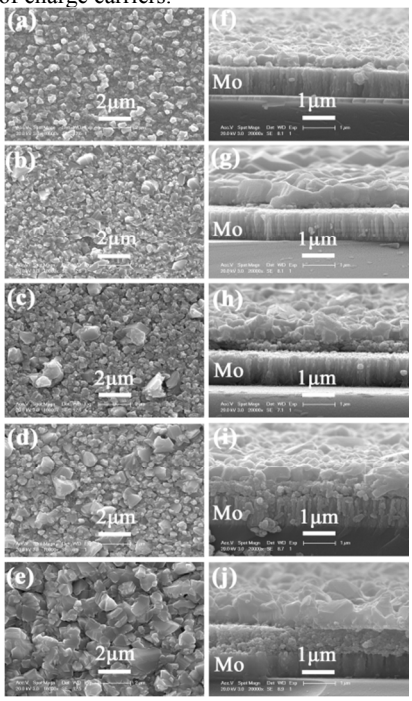

Fig. 2 Surface and cross sectional SEM images of the sulfurized CZTS films deposited for different durations: (a, f) CZTS(05), (b, g) CZTS(10), (c, h) CZTS(20), (d, i) CZTS(30) and (e, j) CZTS(40).

The cross-section images of the CZTS films are shown in Fig. 2(f, g, h and j). The thickness of the films increases quasi-linearly from 0.35 μm for CZTS(05) film, to 0.8 μm, 1.1 μm, 1.2 μm and 1.85 μm for CZTS(10, 20, 30 and 40) films, respectively. The MoS_2 layer is not observed between the CZTS film and the Mo back contact interface. When the deposition time increases from 5 to 10 min, uniform fine grains with homogeneous and densely-packed morphology are formed in Fig. 2(f and g). However, further increase in deposition time above 20 min, the films consist of a bi-layered structure: a large-grain top layer and a small-grain bottom layer in Fig. 2(h, i and j). The small-grain bottom layer indicates that sufficient sulfurization is not achieved, this can be explained by the fact that sulfur is difficultly incorporated into the relatively thick CZTS precursors to form CZTS(20, 30 and 40) films with severely S-poor compared with CZTS(05 and 10) films with obviously S-rich, as presented in Table S1 (ESI†). The small-grain sizes are generally deleterious to device performance due to increased opportunity for recombination between neighboring small particles. Hence, it would be an optimum sulfurization temperature and/or sulfurization duration to achieve a homogeneous and large densely packed grains for CZTS absorber.

The chemical compositions of all sulfurized CZTS films are shown in Table S1 (ESI†). The contents of Cu, Zn and Sn increase while that of S decreases in all CZTS films, which reveals that S is sufficiently incorporated into very thin films to form CZTS during sulfurization. The (05 and 10) films are non-stoichiometry which may result from the high population of intrinsic defects. Interestingly, the CZTS(20 and 30) films have Cu-poor and Zn-rich growth condition which may give superior photovoltaic performance.[3,5,11] However, for the CZTS (40) film, it is Cu-rich and Zn-rich, and the compositional deviation from stoichiometry is not severe.

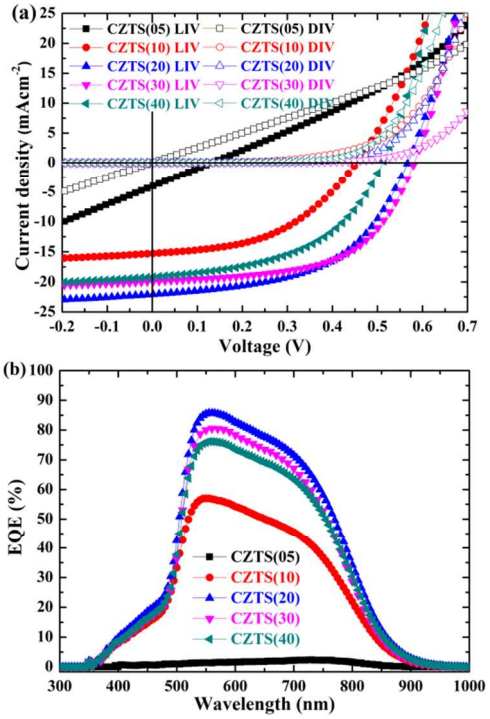

Fig. 3(a) J-V characteristics of the CZTS solar cells with a 150 nm-thick sputtered CdS measured in dark and under AM1.5 simulated illumination. (b) EQE measurements of the corresponding CZTS solar cells.

The comparison of current-voltage (J-V) characteristics for the CZTS solar cells using two different thick sputtered CdS buffer layers (150 nm and 170 nm) are shown in Fig. 3a and Fig. S1a (ESI†). Table S2 and Table S3 (ESI†) show their parameters in J-V characteristics. A short circuit current density (J_{sc}) of 22.0 mA cm^{-2} is obtained from the CZTS(20) cell with a CdS thickness of 150 nm. This reaches the highest J_{sc} ever reported for CZTS solar cells.[2] When compared with the J_{sc} (18.2 mA cm^{-2}) of the CZTS(20) cell with a 170 nm thick CdS buffer layer, the relative J_{sc} enhancement for the CZTS(20) cell with a 150 nm thick CdS buffer layer is ~20%. Such an increase in J_{sc} may be attributed to the light below 520 nm easily through the relatively thin sputtered CdS into the CZTS absorber, as seen in EQE analysis (Fig. 3b and Fig. S1b (ESI†)). As increase deposition time, CZTS(20) and CZTS(30) solar cells have the best efficiency 6.6%. The improvement originates from the boost of J_{sc} from 4.1 to 22.0 mA cm^{-2}, V_{oc} from 133.2 to 581.4 mV and fill factor (FF) from 25.1 to and 57.2%. The significant improvement of V_{oc}, J_{sc} and FF can be mainly attributed to the increment in the suitable thickness of the CZTS absorbers with large grains in combination with the SEM results in Fig. 2. Further increase in deposition time to 30 min, the larger grain results in higher V_{oc}; however, the efficiency is not obviously improved. This is due to the decrease in J_{sc} which counterbalances the increase in V_{oc}. A possible cause for a low J_{sc} value obtained in CZTS(30) solar cell is due to the small-grain bottom layer which becomes thicker, as shown in Fig. 2. When the deposition time increases from 20 to 30 min, V_{oc} improves from 567.0 to 581.4 mV. It is well known that $V_{oc} \propto (AkT/q)\ln(J_{sc}/J_o)$, where A, kT/q and J_o are the diode ideality factor, thermal voltage and reverse saturation current, respectively. Table S2 (ESI†) shows that J_o values of CZTS(20) and CZTS(30) are 5.93 $\times 10^{-4}$ and 9.33×10^{-5} mA cm^{-2}, respectively. V_{oc} is inversely proportional to J_o and thus CZTS(30) has a bigger V_{oc} value that CZTS(20). Moreover, R_{sh} value of CZTS(30) is relatively higher than that of CZTS(20), as seen in Table S2 (ESI†). Consequently higher R_{sh} can also give rise to higher V_{oc}. The CZTS solar cell obtained from CZTS(30) absorber gives the best η value of 6.6% with V_{oc} (581.4 mV), J_{sc} (19.9 mA cm^{-2}), fill factor (FF=57.2%) and series resistance (R_s=5.3 Ω cm^2), respectively. This is the highest reported efficiency obtained for a co-electrodeposited CZTS solar cell to date. However, the low shunt resistance (R_{sh}=282.8 Ω cm^2) comparable with that reported for a champion electrodeposited CZTS solar cell,[2] indicates that there may be some leaks or a voltage-dependent current collection in the device. The cross-over behavior observed in the electrodeposited,[2] hydrazine-processed[3] and co-evaporated[6] CZTS devices, and might be associated with the presence of an electrical barrier either in the buffer/absorber interface or in the back contact.[16] Therefore, it is suggested that this barrier is highly likely responsible for higher series resistance in the devices.

It clear that the J-V curve of the CZTS(05) solar cell exhibits an almost ohmic behavior with low η, V_{oc}, J_{sc} and FF values, as shown in Fig. 3a. As discussed above, a very thin CZTS absorber with small grain size should induce significant cell leakage current. On the other hand, CZTS(10) and CZTS(20) solar cells have appreciable performance. The CZTS(20) solar cell exhibits better performance, with η of 6.6%, J_{sc} of 22.0 mA cm^{-2}, V_{oc} of 567.0 mV and FF of 52.8%, than that of the CZTS(10) cell (η=3.3%, J_{sc}=15.2 mA cm^{-2}, V_{oc}=453.1 mV and FF=47.1%). As can be seen in Fig. 3a, the J-V curve of the CZTS(10) solar cell shows relatively poor electrical rectification with a low R_{sh} (117.3 Ω cm^2) and a high R_s (9.9 Ω cm^2). The thinner CZTS(10) film (Fig. 2g) leads to the generation of an appreciable shunt pass: the low R_{sh} significantly reduces V_{oc}. Moreover, the resulting high R_s leads to a drop in the FF value as well as a decrease in J_{sc}. In contrast, the CZTS(20) solar cell shows relatively good electrical rectification, as can be seen in Fig. 3a. Significant improvement in V_{oc} is due to the appropriate thick CZTS absorber and large grain size, which leads to suppression of shunting: it has a relatively high R_{sh} (183.1 Ω cm^2). The enhancement of J_{sc} and FF are directly related to the decrease in the R_s (5.9 Ω cm^2). The solar cells (C1-15) are other devices in the CZTS(20) and CZTS(30) samples which are close to the best CZTS solar cell (6.6%) in Table S4 (ESI†). This result indicates a relatively well-controlled composition distribution in the CZTS absorber. Compared to the CZTS(20) solar cell, the characteristics of the CZTS(40) solar cell is limited by low J_{sc}, V_{oc} and FF possibly due to the very thick CZTS absorber and rather rougher surface increasing the interface combination of charge carriers and an obvious bi-layered structure with small grains leading to the shunting path between the CZTS and the Mo electrode in Fig. 2j. The effect of deposition time on absorber properties and device performance have been confirmed by different batches of repeated experiments.

Fig. 3b and Fig. S1b (ESI†) show the external quantum efficiency (EQE) of the corresponding CZTS solar cells with the two different thick sputtered CdS films as a function of photon wavelength. When the deposition time increases from 5 to 20 min, the maximum EQEs for CZTS solar cells increase from ~3% to ~85% at 560 nm (Fig. 3b). The band gap of the CZTS(20) extracted from the EQE data is about 1.48 eV (Fig. S3, ESI†), which is close to that of the reported kesterite CZTS device.[4] The EQE value of CZTS(20) solar cell with a CdS thickness of 150 nm is higher than that with a CdS thickness of 170 nm (Fig. S4, ESI†), which is consistent with the higher J_{sc} in combination with in Table S2 and Table S3 (ESI†). The loss in the EQE for wavelengths below ~520 nm is caused by the absorption in the CdS layer, showing the large potential for further improvement in J_{sc} and η by properly reducing the thickness of the CdS layer. This result is similar to the semi-empirical optical modeling done for CZTSSe solar cells.[15] On the other hand, in the wavelength region from 520 to 1000 nm, the EQE

value of the CZTS solar cell from CZTS(20) absorber is higher than that from other absorbers. This can be explained by the fact that the CZTS(20) absorber from relatively long deposition time has better quality: larger grains with less grain boundaries, no obvious bi-layered structure and a suitable absorption thickness. The EQEs in the visible range gradually decays for longer wavelength. The loss at longer wavelength is likely caused by a short minority carrier diffusion length.[2,3,14]

In conclusion, high-performance CZTS solar cells with a maximum η of 6.6% have been fabricated by a sputtered CdS buffer layer for the first time. It is found that the increase in deposition time from 5 to 30 min can quasi-linearly increase the thickness and micron-sized grain, significantly improves the crystallinity of the absorber, greatly reduces the series resistance, and consequently improves the device efficiency greatly by the boost of J_{sc} and V_{oc}. However, the further increase of the deposition time to 40 min, the excessive increase in the thickness of the CZTS absorber leads to some degradation in different device parameters. It is necessary to control the electrodeposition time to ensure CZTS absorber with large grain size and appropriate film thickness.

This project was financed by the National Science Foundation of China (61106064, 61376129 and 61474045), the State Key Basic Research Program of China (2013CB922300) and Knowledge Innovation Program of the Chinese Academy of Sciences (Grant No. Y2K4401DG0).

Notes and references

[a] Key Laboratory of Polar Materials and Devices, Ministry of Education, Department of Electronic Engineering, East China Normal University, Shanghai 200241, China. E-mail address: lsun@ee.ecnu.edu.cn; Fax: +86 21 54345119; Tel.: +86 21 54345157

[b] National Laboratory for Infrared Physics, Shanghai Institute of Technical Physics, Chinese Academy of Sciences, Shanghai 200083, China

† Electronic supplementary information (ESI) available: Experimental details, composition analysis, additional J-V characteristics and band-gap energy determination.

1 A. Khare, A. W. Wills, L. M. Ammerman, D. J. Norrisz and E. S. Aydil, Chem. Commun., 2011, 47, 11721-11723.

2 S. Ahmed, K. B. Reuter, O. Gunawan, L. Guo, L. T. Romankiw and H. Deligianni, Adv. Energy Mater., 2012, 2, 253-259.

3 T. K. Todorov, J. Tang, S. Bag, O. Gunawan, T. Gokmen , Y. Zhu and D. B. Mitzi, Adv. Energy Mater., 2013, 3, 34-38.

4 K. Woo, Y. Kim and J. Moon, Energy Environ. Sci., 2012, 5, 5340-5345.

5 W. Wang, M. T. Winkler, O. Gunawan, T. Gokmen, T. K. Todorov, Y. Zhu and D. B. Mitzi, Adv. Energy Mater., 2014, 4, 1301465.

6 B. Shin, O. Gunawan, Y. Zhu, N. A. Bojarczuk, S.J. Chey and S. Guha, Prog. Photovolt: Res. Appl., 2013, 21, 72-76.

7 H. Katagiri, K. Jimbo, W. S. Maw, K. Oishi, M. Yamazaki, H. Araki and A. Takeuchi, Thin Solid Films, 2009, 517, 2455-2460.

8 Z. Su, K. Sun, Z. Han, H. Cui, F. Liu, Y. Lai, Y. Lai, J. Li, X. Hao, Y. Liu and M. A. Green, J. Mater. Chem. A, 2014, 2, 500-509.

9 F. Liu, K. Sun, W. Li, C. Yan, H. Cui, L. Jiang, X. Hao and M. A. Green, Appl. Phys. Lett., 2014, 104, 051105.

10 S. Exarhos, K. N. Bozhilov and L. Mangolini, Chem. Commun., 2014, 50, 11366-11369.

11 F. Jiang, S. Ikeda, T. Harada and M. Matsumura, Adv. Energy Mater., 2014, 4, 1301381.

12 A. Ennaoui, M. Lux-Steiner, A. Weber, D. Abou-Ras, I. Kötschau, H.-W. Schock, R. Schurr, A. Hölzing, S. Jost, R. Hock, T.Voß, J. Schulze and A. Kirbs, Thin Solid Films, 2009, 517, 2511-2514.

13 J. Tao, J. He, K. Zhang, J. Liu, J. Jiang, Y. Dong, L. Sun, P. Yang and J. Chu, Mater. Lett., 2014, 135, 8-10.

14 Y. Lin, S. Ikeda, W. Septina, Y. Kawasaki, T. Harada and M. Matsumura, Sol. Energy Mater. Sol. Cells, 2014, 120, 218-225.

15 M. T. Winkler, W. Wang, O. Gunawan, H. J. Hovel, T. K. Todorov and D. B. Mitzi, Energy Environ. Sci., 2014, 7, 1029-1036.

16 G. Agostinelli, D.L. Batzner, M. Burgelman, Thin Solid Films, 2003, 407, 431-432.

